Spoof surface plasmon polaritons excited leaky-wave antenna with continuous scanning range from endfire to forward

Tao Zhong(钟涛)† and Hou Zhang(张厚)

Air and Missile Defense College, Air Force Engineering University, Xi'an 710051, *China*

(Received 23 May 2020; revised manuscript received 4 June 2020; accepted manuscript online 12 June 2020)

A novel leaky-wave antenna (LWA) utilizing spoof surface plasmon polaritons (SSPPs) excitation is proposed with continuous scanning range from endfire to forward. The designed transmission line unit supports two SSPPS modes, of which the 2nd order mode is applied in the design. A novel strategy has been devised to excite the spatial radiation of the −1st order harmonics by arranging periodic counter changed sinusoidal structures on both sides of the SSPPs transmission line. Both full-wave simulation and measurement results show that the proposed LWA presents wide scanning angle from endfire to forward. In the frequency range from 4 GHz to 10 GHz, LWAs achieve scanning from 90° to +20°, covering the entire backward quadrant continuously.

Keywords: leaky-wave antenna, spoof surface plasmon polaritons, wide scanning-angle

PACS: 41.20.Jb, 84.40.–x, 84.40.Ba **DOI:** 10.1088/1674-1056/ab9c00

1. Introduction

Leaky-wave antenna (LWA) is a guiding structure that possesses a mechanism that allows a traveling wave to leak its power along the structure length.[1] Compared to traditional array antennas, they are widely appreciated because of their simple easy-feeding network, high gain low cost, and convenient beam scanning.[1,2] Since it was first proposed,[3] LWAs have undergone more than 70 years of development, with forms ranging from rectangular waveguides to planar microstrips, to the current emerging electromagnetic structures.[4–9] In general, LWAs are divided into uniform and periodic structures.[10] The uniform structure of the LWA is simple, but has a significant limitation in the scanning range and can only perform forward scanning. Periodic LWAs are capable of backward-to-forward continuous scanning, but few literature reports implement LWAs with endfire scanning. In Ref. [11], a continuous sweep from endfire direction to forward direction is achieved based on the Goubau line. While this work has clear advantages in terms of scanning range, it falls short in terms of size. The spoof surface plasmon polaritons (SSPPs) transmission line proposed in recent years offers some new approaches to the design of LWA

Surface plasmon polaritons (SPPs) are localized or propagating surface electromagnetic waves in which photons collectively oscillate with free electrons in the interfacing metal.[12] The concept of SSPPs comes from SPPs in optics, which is electromagnetic features similar to those of SPPs by constructing special structures that bound electromagnetic waves to the surface of the medium, or force them to travel along the surface. In 2012, SSPPs transmission lines have evolved from their previous three-dimensional structure into a planar structure, significantly improving their integration capabilities and range of applications.[13,14] Subsequently, SSPPs have been widely used in electronic components,[15] and LWAs are no exception.[16–18] In Ref. [16], the means of applying SSPPs to antenna radiation are systematically summarized. In Ref. [17], frequency scanning radiation from 4.8° to 37.2° is realized by decoupling SSPPs utilizing phase gradient metasurface. In Ref. [19], using the principle of electromagnetic coupling, an LWA with −45° to 45° continuous scanning is achieved by loading circular patches on both sides of the SSPPS transmission line. Nonetheless, the LWAs proposed based on these literatures are deficient in the beam scanning range, and new design approaches are highly desirable to extend the beam scanning range.

In this paper, an LWA based on SSPPs excitation is proposed with continuous scanning range from endfire to forward. First, a novel type of SSPPs supported transmission line is proposed, and the dispersion characteristics of the unit cell are analyzed at the same time. Then, a periodic sinusoidal modulation structure is loaded on the base of the transmission line to excite the −1-order harmonics and form electromagnetic radiation. Lastly, the optimized simulation model fabrication and the prototype measurement are carried out to verify the correctness of the design.

2. Design of LWA and analysis

Figure 1 shows the configurations of the proposed LWA based on SSPPs excitation transmission line. The LWA proposed in this paper is composed of three components, corresponding to the coplanar waveguide (CPW) feeding part, CPW to SSPP transiting part and SSPP energy radiating part,

†Corresponding author. E-mail: ztbull@126.com

as shown in Fig. 1(a). The electromagnetic wave is converted from CPW transmission mode to SSPPs transmission mode owing to the conversion structure. An asymmetrical uninterrupted winding slot is engraved in the transmission line part, and gradually varied length is applied to meet impedance conditions.

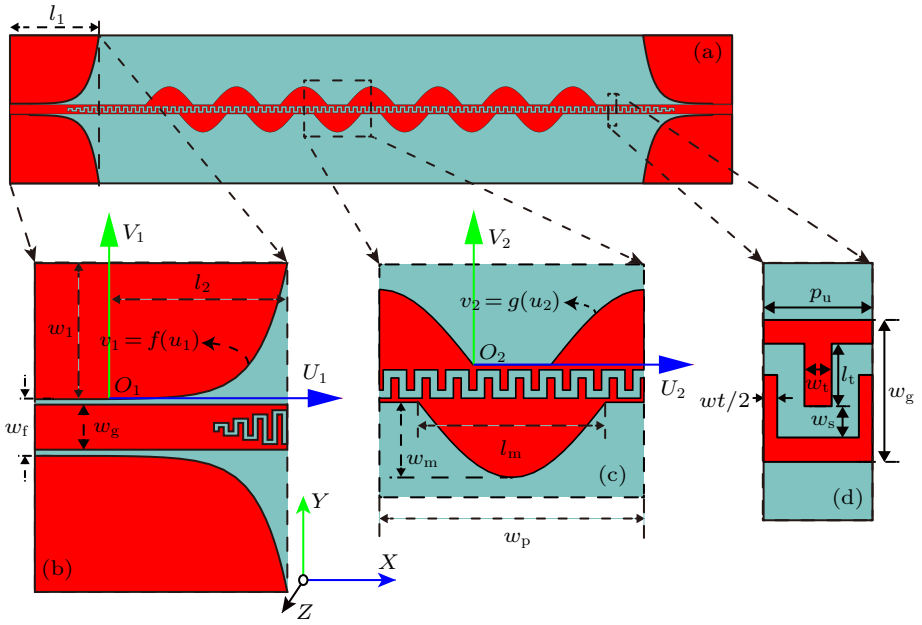

Fig. 1. Configurations of the proposed LWA based on SSPPs excitation transmission line. (a) Top view of proposed LWA. (b) Details of the feeding and transiting part. (c) Details of the radiating part. (d) Unit cell of transmission line.

To better describe the configurations, the details of the LWA are shown in Fig. 1(b) and Fig. 1(c). Reference coordinate system $U_1O_1V_1$ and $U_2O_2V_2$ are built to describe the nonlinear part of the LWA structure. For $U_1O_1V_1$ as shown in Fig. 1(b), the original point of $U_1O_1V_1$ is arranged at the start point of the conversion transition. The outline of conversion transition is determined by the exponential function $v_1 = f(u_1)$

$$f(u_1) = \frac{w_1\left(\mathrm{e}^{au_1} - 1\right)}{\mathrm{e}^{al_2} - 1}, \quad 0 \le u_1 \le l_2, \tag{1}$$

where the parameter a is applied to control the smoothness of outline curve. The relevant parameters of the exponential function should be optimized to get a good transmission.

For $U_2O_2V_2$ as shown in Fig. 1(c), the original point of $U_2O_2V_2$ is arranged at the end point of the unit modulation structure. The outline of unit modulation structure is determined by the piecewise function $v_2 = g(u_2)$,

$$g(u_2) = \begin{cases} 0, & 0 \le u_2 \le l_\mathrm{m}, \\ w_\mathrm{m} \sin\left(\dfrac{\pi(u_2 - l_\mathrm{m})}{w_p - l_\mathrm{m}}\right), & l_\mathrm{m} \le u_2 \le w_\mathrm{p}, \end{cases} \tag{2}$$

where periodic sinusoidal modulated structure is adopted with amplitude w_m.

Some previous research about sinusoidal modulated has shown the great advantages in the synthesis of radiation patterns. On the other hand, the loading of the sinusoidal modulated structure introduces relatively smooth structural change that is beneficial for impedance matching. The relevant parameters of the function $v_2 = g(u_2)$ have been optimized to get a high-efficiency radiation.

The structures of sinusoidal modulation, 13 in total, are distributed on both sides of the transmission line in a central symmetrical manner. The dielectric medium of the LWA is Roger RT5880 with a thickness of 1 mm ($\varepsilon_\mathrm{r} = 2.2$ and $\tan\delta = 0.001$). The corresponding parameter values in the antenna structure are respectively as follows: $w_\mathrm{f} = 5$ mm, $w_\mathrm{g} = 4$ mm, $w_1 = 30$ mm, $l_1 = 10$ mm, $l_2 = 35$ mm, $w_\mathrm{m} = 8$ mm, $l_\mathrm{m} = 24$ mm, $w_\mathrm{p} = 34$ mm, $a = 5$.

2.1. Analysis of SSPPs transmission line

First, the relevant characteristics of SSPPs transmission line are studied. The diagrammatic drawing of the transmission line unit cell is shown in Fig. 1(a). The electromagnetic model of the unit cell is built in the CST microwave studio, as shown in Fig. 2(b). The parameters values for the unit cell in millimeter are listed in Table 1. Eigenmode solver is applied to analyze dispersion characteristics of TL unit cell. In Fig. 3, the dispersion curves of the two fundamental modes of SSPPs are demonstrated. It can be seen from the curves that the dispersion curves of the two modes of SSPPs are not consistent, and the dispersion of the electromagnetic waves in the 1st mode is more pronounced within the operating frequency. In other words, at the same frequency, the phase velocity of an electromagnetic wave in 1st mode is greater than the phase velocity of 2nd mode. The phase constants of modes 1 and 2 are greater than β_air, where β_air is the phase constant in free

space. Therefore, both transmission modes are slow waves. It should be noticed that the slow wave can not radiate due to the momentum mismatch with the electromagnetic wave in the air. By adjusting the structural parameter l_t, the length of the meandering branch of the slot has a significant effect on the dispersion level of the transmission unit cell. For electromagnetic fields of the same mode, the longer the branches, the larger the changing rate of the phase constant with the frequency. In other words, the longer the branch, the more pronounced the dispersion will be.

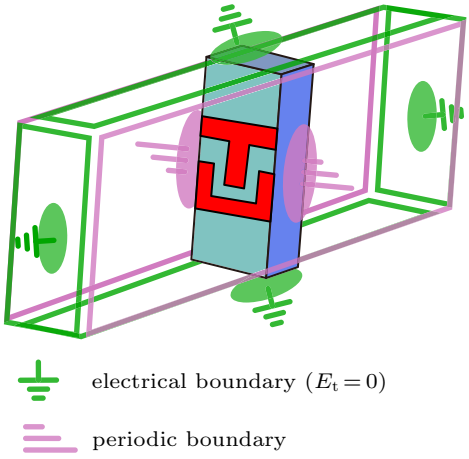

Fig. 2. The electromagnetic model of the transmission line unit cell in simulated condition.

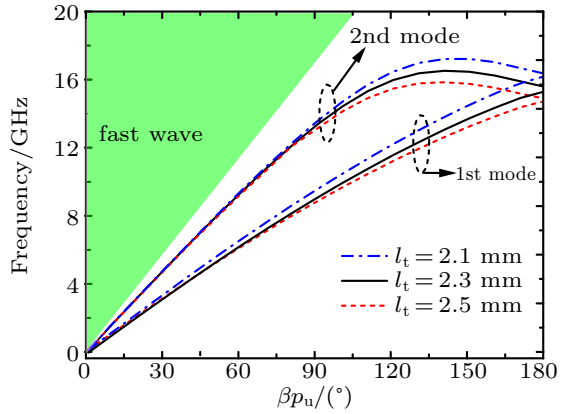

Fig. 3. Dispersion diagram of SSPPs transmission line unit cell with varying structural parameters.

Table 1. Parameters values for the unit cell in unit mm.

Parameters	p_u	w_g	w_t	w_s	l_t
Value/mm	4.4	2.8	1	1.2	2.3

To explore the differences between the two modes, the current distributions on the cell structure under the two fundamental modes are shown in Fig. 4. In the case of 1st mode, the current on both sides of the winding groove flows in the opposite direction, while the current is homodromous in 2nd mode. Although the transmission unit supports two modes of electromagnetic waves, the mode in the corresponding transmission line is also closely related to the transmission line feeding structure. In this paper, a coplanar waveguide feed is used, and the electromagnetic waves excited are symmetrical in mode; therefore, the electromagnetic waves utilized in the transmission line are based on 2nd mode.

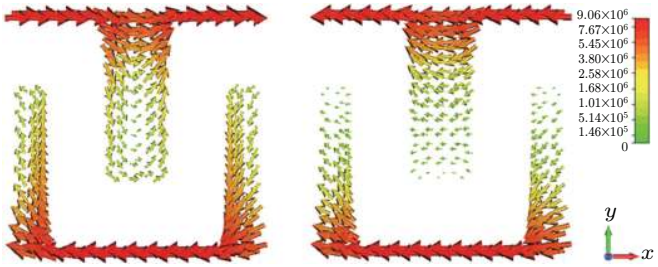

Fig. 4. Surface current distributions of the two fundamental modes: (a) 1st mode, (b) 2nd mode.

2.2. The mechanism of leaky wave radiation

Without losing generality, the slow wave will only conduct along the transmission line and will not radiate due to momentum mismatch. Therefore, the countermeasures should be taken to convert slow waves to fast waves and radiate out. The transmission constant analysis is the first step in the research of LWA characteristic. The propagation constant along the SSPPs transmission line k_x can be described as $k_x = \beta(\omega) + j\alpha(\omega)$ with a phase constant $\beta(\omega)$ and a leakage constant $\alpha(\omega)$. The direction of beam scanning is a function of the operating frequency,[10] as shown by the following formula:

$$\theta_b(\omega) = \arcsin\left(\frac{\beta(\omega)}{k_0}\right). \tag{3}$$

According to the Floquet theory,[16] the electromagnetic field of a transmission line is characterized by an infinite number of spatial harmonics, and the phase constant corresponding to the n-th ($n = 0, \pm1, \pm2, \ldots$) spatial harmonic can be expressed as

$$\beta_n(\omega) = \beta_0(\omega) + \frac{2n\pi}{p}. \tag{4}$$

In formula (4), the parameter p represents the period of the electromagnetic structure, and β is the propagation phase constant for the fundamental mode. As shown in Fig. 1, the structure of sinusoidal modulation is distributed on both sides of the transmission line, which is bound to excite the high-mode harmonics. Typically, the 1st harmonics are excited and produce radiation. Thus, combining formulas (3) and (4), the beam pointing of the proposed LWA radiation can be obtained as

$$\theta_b(\omega) = \arcsin\left(\frac{\beta_0(\omega)}{k_0} - \frac{2\pi}{k_0 p}\right). \tag{5}$$

3. Numerical and experimental results

To validate the design, a prototype of the LWA is fabricated and measured, as shown in Fig. 5. The dielectric medium of the proposed LWA is Roger RT5880 with a thickness of 1 mm ($\varepsilon_r = 2.2$ and $\tan\delta = 0.001$). The overall size of the LWA is 365 mm×65 mm. The N5230C vector network analyzer is used to measure the scattering parameters, and the normalized radiation patterns are measured in a microwave anechoic chamber. In the measurements, it should be noted that, as a two-port device, one port of the LWA is connected to the signal source and the other port to a 50-Ω matching resistor. The normalized patterns of the LWA are characterized by the changing law of the receiving electromagnetic wave energy. A standardized gain antenna is used to the measurement of the LWA gain as shown in Fig. 8. The gain of the LWA can be obtained by comparing the strength of the signal emitted by the standard antenna and the LWA. The ratio of the received signal strength is equal to the ratio of the corresponding transmitting antenna gain. The comparisons between the measured and simulated results are given in Figs. 6–8.

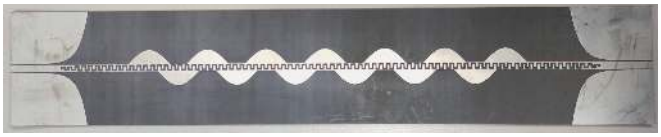

Fig. 5. Photograph of the fabricated sample.

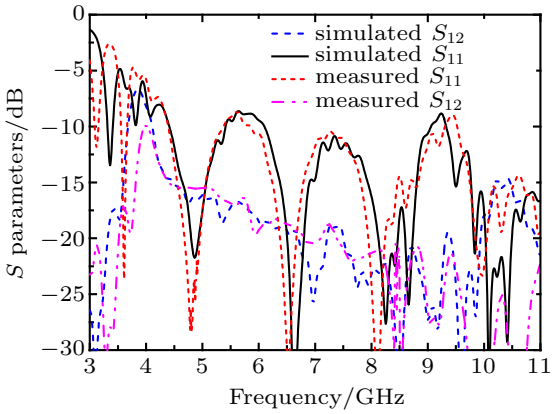

Fig. 6. The simulated and measured S-parameters of the proposed LWA.

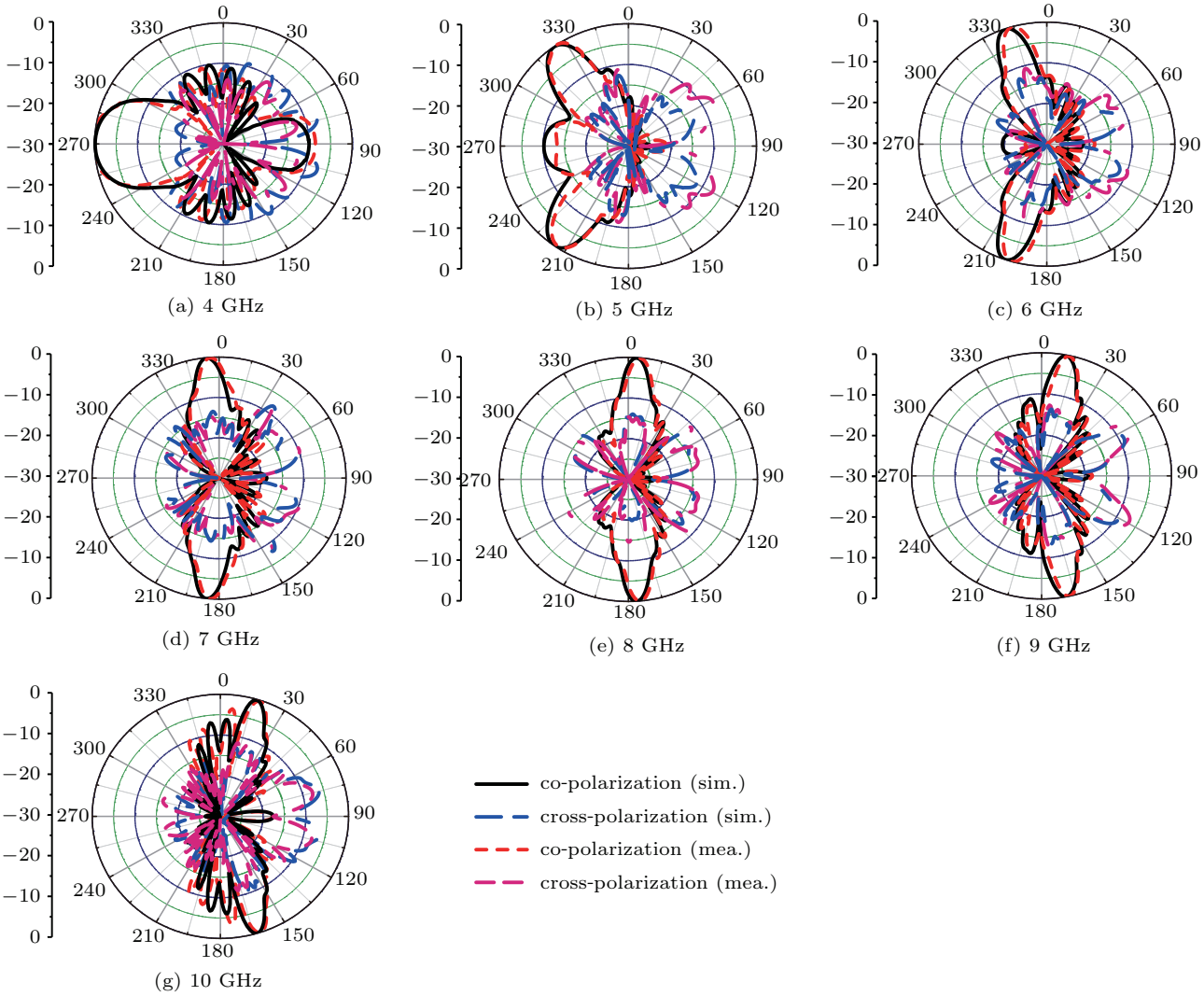

Fig. 7. The simulated and measured normalized radiation patterns of the proposed LWA: (a) 4 GHz, (b) 5 GHz, (c) 6 GHz, (d) 7 GHz, (e) 8 GHz, (f) 9 GHz, (g) 10 GHz.

The simulated and measured *S*-parameters of the proposed LWA are plotted in Fig. 6. Although the frequency is slightly offset due to media loss and the measurement environment, the measured and simulated results match each other well within the operating frequency range. The scattering parameters of the antenna are maintained at a low level in the operating frequency range, which indicates that most of the feed-in energy is converted to space radiation and heat loss.

The measured and simulated normalized radiation patterns at 1-GHz interval from 4 GHz to 10 GHz are shown in Fig. 7, which illustrates the relationship of the antenna beam pointing with frequency on the scanning plane, as well as the features of co-polarization, cross-polarization, and sidelobe. As can be seen in Fig. 7(a), the LWA is radiated in the endfire direction at 4 GHz. As the frequency increases, the LWA beam changes continuously from endfire to forward until it reaches 20° forward at 10 GHz. It should be noted that at around 7.5 GHz, the antenna beam is radiated at the broadside direction and has a good performance, which indicates that the antenna mitigates the open-stopband well. The cross-polarization of the LWA is also given out in Fig. 7. The cross-polarization of the LWA is at a low level within the operating frequency range, illustrating that the LWA has good polarization isolation.

Figure 8 illustrates the curves of the LWA for realized gain and beam pointing *versus* frequency. At around 4.2 GHz, there is a significant drop in the realized gain of the LWA, which is attributed to the splitting of the beam, with the pencil beam evolving into a conical beam. Simulated and measured results show that the antenna achieves a wide scan range from endfire end to forward, covering the entire backward quadrant. The realized gain of the antenna is slightly fluctuating in the high frequency band, but remains above 8 dB overall. At 8.4 GHz, the simulated achieves a maximum realized gain of 10.2 dB.

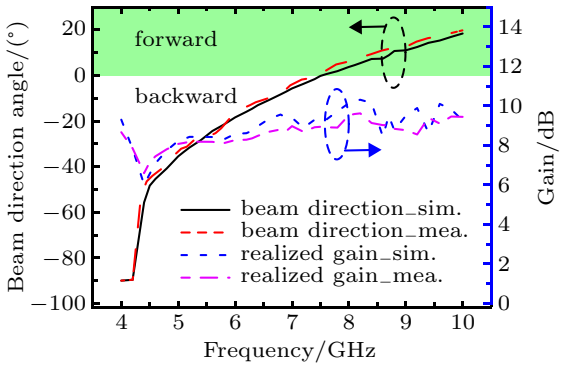

Fig. 8. The simulated and measured beam direction angle and realized gain of the proposed LWA.

Table 2. Performances comparing between the LWA and previous works.

Works	Antenna type	Length/mm	Operating frequency/GHz	Scanning range/(°)
Ref. [7]	QMSIW	230	8.9 to 11.8	−43 to 32
Ref. [8]	Goubau-line	292	9.0 to 13	−13.1 to 19.1
Ref. [9]	Microstrip line	171	10.7 to 17	−78 to 27
Ref. [17]	SSPPs	297	8.8 to 10.7	4.8 to 37.2
Ref. [18]	SSPPs	320	5 to 11	−45 to 10
Ref. [20]	HMSIW	46	55 to 65	−72 to 48
This work	SSPPs	365	4.0 to 10	90 to 20

Table 2 compares the performance of the proposed antennas with works that already exist in other literatures. The greatest feature of the work in this paper is that the beam scan angle covers the endfire direction which is difficult to realize in LWA design. At the same time, the LWA's scanning range of 110° is better than most other LWAs, which greatly expands the range of applications

4. Conclusion

A novel LWA with wide scanning angle is designed, fabricated, and measured in this paper. The relevant dispersion characteristics of the transmission line and the working principle of the LWA are described. The measured and simulated results of the designed LWA are in good agreement with each other, indicating that a continuous beam scanning range from endfire to forward over the operating frequency band of 4 GHz–10 GHz is obtained. This work provides a novel and wonderful way to design LWAs with wide-scanning beam, further expanding the application of SSPPs.

Acknowledgment

The authors would like to express their gratitude to the China North Electronic Engineering Research Institute for their contribution to the fabrication of LWA prototype.

References

[1] Jackson D R, Caloz C and Itoh T 2012 *Proc. IEEE* **100** 2194

[2] Constantine A B 2008 *Modern Antenna Handbook* (Hoboken: John Wiley & Sons, Inc.) p. 325

[3] Hansen W W (U.S. Patent) 2402622 [1940]

[4] Jackson D R, Baccarelli P, Burghignoli P, Fuscaldo W, Galli A and Lovat G 2019 *URSI International Symposium on Electromagnetic Theory*, May 27–31, 2019, San Diego, CA, USA, p. 1
[5] Jackson D R and Oliner A A 1988 *IEEE Trans. Antennas Propag.* **36** 905
[6] Caloz C, Itoh T and Rennings A 2008 *IEEE Anten. Propag. M.* **50** 25
[7] Wu G C, Wang G M, Fu X L, Liang J G and Bai W X 2017 *Chin. Phys. B* **26** 024102
[8] Tang X L, Zhang Q F, Hu S M, Zhuang Y Q, Kandwal A, Zhang G and Chen Y F 2017 *Sci. Rep.* **7** 11685
[9] Tiwari A K, Awasthi S and Singh R K 2020 *IEEE Anten. Wireless Propag. Lett.* **19** 646
[10] Xu F and Wu K 2013 *IEEE Microw. Mag.* **14** 87
[11] Rudramuni K, Kandasamy K, Zhang Q, Tang X L, Kandwal A, Rajanna P K T and Liu H 2018 *IEEE Anten. Wireless Propag. Lett.* **17** 1571
[12] Zhu W R, Rukhlenko I D and Premaratne M 2013 *Appl. Phys. Lett.* **102** 011910
[13] Liao M L, Wei Y Y, Wang H L Huang Y Xu J, Liu Y, Guo G, Niu X J, Gong Y B and Park G S 2016 *Chin. Phys. Lett.* **33** 90701
[14] Shen X P, Cui T J, Martin-Cano D, and Garcia-Vidal F J 2013 *Proc. Natl. Acad. Sci. USA* **110** 40
[15] Zhang H C, He P H, Tang W X, Luo Y and Cui T J 2019 *IEEE Microw. Mag.* **20** 73
[16] Tang W X, Cui T J 2019 *EPJ Appl. Metamat.* **6** 9
[17] Fan Y, Wang J F, Li Y F, Zhang J Q, Qu S B, Han Y J, and Chen H Y 2018 *IEEE Trans. Anten. Propag.* **66** 203
[18] Yin J Y, Ren J, Zhang Q Zhang H C, Liu Y Q, Li Y B, Wan X and Cui T J 2016 *IEEE Trans. Anten. Propag.* **64** 5181
[19] Liu L L, Wang J, Yin X X and Chen Z N 2018 *Electronics* **7** 348
[20] Sarkar A and Lim S 2020 *IEEE Trans. Anten. Propag.* **68** 5816